RESEARCH ARTICLE

Journal of Medical Imaging and Health Informatics
Vol. 6, 1020–1026, 2016

Analysis of Healthy versus Tumor Pixels Based on Segmentation Techniques for High Intensity Focused Ultrasound Interventions

P. Revathy* and V. Sadasivam

Department of Computer Science and Engineering, PSN College of Engineering and Technology, Tirunelveli 627152, India

Liver cancer is one of the causes of cancer death worldwide. Medical imaging has found its way in diagnosing the liver cancer by various imaging modalities. High Intensity Focused Ultrasound is one of the latest noninvasive heat based imaging technique for treating liver cancer. In this research paper the input CT image of a tumorous liver is taken for analysis. The input image is converted to gray scale intensities and plotted in a matrix format. In the preprocessing stage two segmentation techniques, the threshold based segmentation and Chan Vese active contours segmentation are used to find the Region of interest. The segmentation results are analyzed. The healthy and the tumor pixels are analyzed for both the segmentation techniques and the results are tabulated. A new pixel wise heat prediction for cancer tissue is used to predict heat to be applied to treat tumor. Further heat to be applied pixel wise is calculated by the ideal heat prediction method using Pennes Bio Heat Transfer Equation and the results are compared with the proposed heat prediction method.

Keywords: Bio-Heat Transfer Equation, Medical Image Processing, High Intensity Focused Ultrasound (HIFU), Threshold Based Segmentation, Chan Vese Active Contours Segmentation.

1. INTRODUCTION

Liver cancer is one of the cause of cancer death worldwide. Different types of cancer treatments are surgery, chemotherapy, radiation therapy, targeted therapy, immunotherapy and hyperthermia. Hyperthermia is a heat treatment in which controlled usage of heat is used to treat cancer tissue. Warmer temperature may heat the cancer tissue and cause results as produced by chemotherapy or radiation therapy. But very high temperature kills the cancer cells.[1] Magnetic resonance guided High Intensity Focused Ultrasound (MRgHIFU) is a non-invasive hyperthermia method that uses non-ionizing radiation for identifying and ablating tumor affected tissues.[2] The surface intensity at the transducer face is very low in the range of 20 to 40 Watts/cm^2 which is required to achieve a very high intensity of 1600 to 2000 Watts/cm^2 at the focal point. Focal point is the place where the significant energy deposition at the focus happens. The temperature within the tissue should be within the range 55 °C to 85 °C to destroy the tumor tissue completely.[3] The method used Pennes Bio-Heat Transfer Equation (PBHTE) is an ideal heat prediction method. This is used to calculate the temperature and the thermal dose fields.[4]

Other heat prediction models are Klinger continuum model and Wulff continuum model. Many different types of computer aided diagnosis schemes are being developed for detection and/or characterization of various lesions in medical imaging. They are conventional projection radiography (CPR), computed tomography (CT), Magnetic resonance imaging (MRI) and Ultrasound. In MRgHIFU the Ultrasound beam is focused on a tissue chosen for ablation and it is guided and controlled using Magnetic Resonance (MR) based thermal imaging.[5] Computer based analysis for cancer treatment using HIFU is desired to provide computable and stable results for assisting the radiologist during treatment planning. Accuracy in thermal dose depends on the results from the Computer aided diagnosis. An accurate dose prevents damage to the nearby organ or tissue. Any abnormal cell that cluster together to form a mass or lump and disturbs the normal functionality of the particular organ in the human body is a tumor. Liver tumor is the abnormal growth in the liver.[6]

The image in Figure 1 shows a model of tumor cells surrounded by healthy cells. Any tumor can be classified as primary or secondary tumor. Tumors that originate in the liver may be benign and malignant known as primary tumors and the tumor that has spread to the liver from its original source of origin in another part of the body is a secondary tumor.

Ablation through HIFU destroys the structure of the tumor cell and therefore the further multiplication of the tumor cell is reduced. After HIFU treatment the healthy cells supports in transforming the ablated cell in to a healthy tissue. The input

*Author to whom correspondence should be addressed.

 2156-7018/2016/6/1020/007 doi:10.1166/jmihi.2016.1784

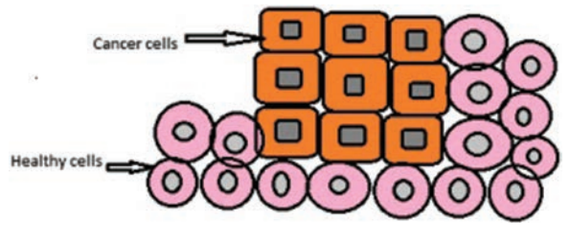

Fig. 1. A model arrangement of cancer cells surrounded by healthy cells.

image taken for analyzing the tumor is a secondary tumor which has originated from colon. Input image is converted to gray scale intensities and plotted in a matrix format and the necessary pixels are analyzed. The tumor region mapped in matrix format is shown in Figure 2. This illustration is about the treatment spots for applying necessary heat in tumor region. The solid box shows the region of particular grey scale intensity. The center grid line shows the center points for heat application during HIFU treatment. The closed region is the lesion or the region of interest where heat prediction is done. By considering the above concept the input image is tabulated in a 200×280 mesh. Mesh is a table of pixel intensity values. Intensities helps to identify the level of tumor infection at that point.

1.1. Similar Research

Variation of temperature distribution was used to identify the abnormality in the infrared images of diseased breasts and improved gradient vector flow snake method was used to detect the boundary of the tumor.[7] Prediction of the risk of developing breast tumor based on thermographs is discussed in this research paper.[8] Color segmentation of thermal infrared breast images is explained in this research paper.[9] A recent work has used the projection profile approach to segment the breast and temperature variation is used to identify the tumorous tissue in the thermogram image.[10] Various techniques for automatic segmentation of tumor in human liver are discussed by Vinita Dixit.[11] When comparing the results of the proposed research with relevant papers, the base temperature is taken as 37 °C by taking the standard value as absorption coefficient for human tissue. Also the temperature at the highly focused region is 65 °C in average

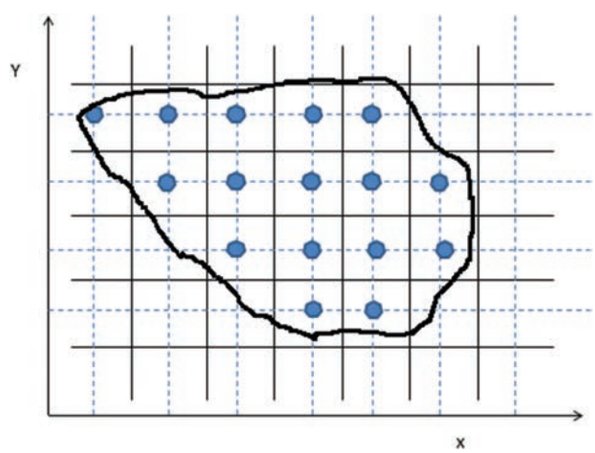

Fig. 2. Illustration of tumor region indicating the spots for applying heat.

and in the off focus regions the temperature is 42 °C.[12] In the proposed research paper the base temperature of human tissue is taken as 37 °C for simulation. And the predicted heat has reached 58.73 °C in an average at the highly focused region. In the region of non interest the average temperature is 39.11 °C. A MRI parameter, Magnetization transfer ratio (MTR) is used to identify the HIFU treated and non-treated tumor tissue. Also the temperature has risen up to 66 °C.[13] The region after applying heat is segmented as above 50 °C, 55 °C, 60 °C. The absolute highest temperature measured for a single pixel was 97.8 °C.[14] In the proposed paper the highest temperature measured for a single pixel was 94.46 °C. In reference paper[15] the author has discussed that good segmentation results were obtained by processing the intensity band of image.

2. PROBLEM FORMULATION

Prediction of heat to be applied for HIFU treatment of abdominal organ like liver affected by tumor using Pennes Bio-heat heat prediction method considers the blood perfusion term as a constant. But the blood vessels passing through the liver carry away the heat to be applied to treat the affected area. Hence complete necrosis cannot be achieved. Also medical images are affected by intensity inhomogeneity, weak boundary, noise and the presence of similar objects close to each other. Segmentation of the tumor region from the liver is challenging.

2.1. Segmentation and Heat Prediction

Segmentation is the preprocessing step in any tumor detection process. In a heat treatment like HIFU the tumor region is segmented first for treatment planning. So proper segmentation of tumor region is important. A very basic segmentation method is intensity based segmentation which is otherwise called as threshold based segmentation. Thresholding type of segmentation can be done either locally or globally. In this research paper global type of segmentation is used for detection of tumor.

The tumor region is distinguished from the background by comparing with the threshold value chosen and then uses binary partition to segment the image. The threshold value is chosen such that the pixels that pass the threshold value are considered as the tumor object pixel and they are assigned with a binary value 1. Other pixels that do not pass the threshold value are assigned with a value 0 and they are the background pixels.[16] The most basic morphological operations used are dilation and erosion. The result of dilation is that, the output pixel is the maximum value of all the pixels in the input pixel's neighborhood. In a binary image, if any of the pixels is set to the value 1, the output pixel is set to 1, and for erosion, the value of the output pixel is the minimum value of all the pixels in the input pixel's neighborhood.[17] Canny edge detection method is a modification of Sobel method.[18] Canny edge detector implements Gaussian in its method to reduce the effect of noise during edge detection. Canny method provides sharpen edge detection compared to other edge detection methods.[19] Another popular method to segment medical images is the Chan Vese Active contour model otherwise called as Active contour model. The initial contour detection is improved by Chan Vese model. This model works well for intensity inhomogeneity images.[20] This method easily identifies the interior contours and also the objects whose boundaries are not defined by gradient. A classical snake model is an

edge detector which detects the edged based on the gradient value of the image.[21] Hence the active volume contour method is used in this research paper to segment the input image.

The heat transfer in the tissue and the temperature rise is modeled based on Pennes Bio-Heat Transfer Equation (PBHTE).[22] Thus the temperature and thermal dose to be applied to the region of interest are calculated. The physical phenomena of the living tissues are studied by the Bio-Heat Transfer Equations (BHTE). The tradition and the basic one is the Pennes bio-heat transfer equation. Other thermal models of bio-heat transfer are the extended and modified versions of the original work of Pennes. The Pennes bio-heat transfer equation for blood perfused tissues is written as,

$$(\rho C_\rho)_t \frac{\partial T_t}{\partial t} = \nabla \cdot (K_t \nabla T_t) + q_p + q_m \quad (1)$$

Where q_p, $q_m = 700$ W/m^3, ρ_t, $(C_\rho)_t$, T_t, K_t, t are the heat convention, metabolic heat transfer, tissue density, specific heat of tissue, temperature of tissue, thermal conductivity and time respectively. The advantage of PBHTE is that it predicts temperature fields and it is used in hyperthermia modeling. The limitation of PBHTE is that it does not consider the effect of the direction of blood flow. The limitation of PBHTE is overcome by Wulff continuum model and Klinger continuum model.[23, 24] Wulff's equation is given as,

$$(\rho C_\rho)_t \frac{\partial T_t}{\partial t} = \nabla \cdot (k_t \nabla T_t) - \rho_b V_h C_b \nabla T_b - \nabla H_b \nabla \phi \quad (2)$$

Where V_h, H_b, ρ_b, C_b and T_t are local mean blood velocity, specific enthalpy of blood, density of blood, specific heat of blood and tissue temperature respectively. The disadvantage of this method is that the local blood mass flux is hard to determine. The disadvantage of Pennes bio-heat model is that it neglects the effect of blood flow within the tissue. To overcome this, in Klinger continuum model the convective heat caused by blood flow in the tissue was considered. Heat source and velocity of blood flow inside tissue was considered and the modified Penne's model equation is written as,

$$(\rho C_\rho)_t \frac{\partial T_t}{\partial t} + (\rho C)_b V_0 \nabla T_t = k \nabla^2 T_t + q_m \quad (3)$$

Where k_t, T_t, q_m and V_0 are the thermal conductivity, tissue temperature (convective heat caused by blood flow inside the tissue), metabolic heat transfer and the non-uniform velocity field respectively. The blood and the tissue parameters[25, 26] and their values are discussed by comparing the Pennes BHTE, Wulff and Klinger and then the proposed model of heat equation is formed.

3. PROBLEM SOLUTION

To overcome the convective heat transfer problem and to predict the temperature in an efficient way, it is proposed to implement thermal dose and temperature prediction method based on varying blood perfusion.

3.1. The Proposed Equation

The blood perfusion rate (ω_b) and the dynamic viscosity of blood (μ) values are added in the calculation of thermal dose for the proposed model. In the existing algorithm the effect of blood flow within the tissue is neglected and so in the proposed algorithm the perfusion rate and viscosity terms are taken into consideration.[27] Equation of the proposed algorithm is,

$$(\rho C)_t \frac{\partial T_t}{\partial t} = k_t \nabla^2 T_t - (\rho C)_b V_h \nabla T_t - (\rho C)_b \nabla T_t (\omega_b - \mu) + q_m \quad (4)$$

Where $V_h = 10.5$ m/s is the average blood velocity, $\omega_b = 0.5$ kg/m$^3 \cdot$s is the perfusion rate of the blood flow and $\mu = 0.004$ kg/m$\cdot$s is the viscosity of blood.

3.2. Healthy and Tumor Pixels in the Region of Interest (ROI)

The tumor region is extracted from an input abdominal CT image. The image is converted to greyscale intensities. The grey scale intensities are tabulated in a mesh of size 200×280. From the input image a mesh of size 5×5 with the grey scale intensity values of the ROI are shown in the Table I. The input CT image of abdomen with tumor is segmented with threshold based segmentation method and Active contour segmentation method.

The ROI is found using both the above said methods and the analysis about pixels are done. The segmentation result using both the threshold based segmentation method and Chan Vese segmentation method is shown in Figures 3(a to c). The input grey scale image is of size 200×280. The canny edge detector is used for edge detection.

The input image is a CT image of abdominal cancer in the liver. The liver has multiple lesions. The Lesions are identified by the segmentation methods. Threshold based segmentation and Chan Vese active contour method has identified almost equal number of lesions. All the lesion values are plotted in a matrix. The lesion values are the intensity levels of the pixels at that point. The lesion values plotted for a particular lesion marked in red is in Figure 4.

The segmented lesion size varies for both thresholds based and Active contour based segmentation. The analysis about the pixels in the ROI for the threshold based segmentation method is tabulated in Table II.

The parameters analyzed are, the lesion size, the average intensity per lesion, number of pixel intensities in the range less than 100, 100 to 200 and greater than 200. All the above parameters are taken for Active contour based segmentation method and the results are tabulated in Table III. Lesion size is the total number of pixels in the selected region. Average intensity per lesion means the average value of the grey level intensity values in the selected region. Total pixel intensity range of a grey image is from 0 to 255.

0 represents the least intensity value black. And 1 represents the highest intensity white. In Figure 5(a) the Lesion values for threshold based segmentation is listed. In Figure 5(b) the lesion values for Active contour method is listed. And in Figure 5(c) the lesion values for both the methods are overlapped. Active contour method has identified the edges more accurately than the threshold based segmentation.

Table I. A 5 × 5 matrix of grey scale intensities from the input image.

255	178	130	118	191
255	158	145	157	173
255	141	163	186	122
187	197	127	122	171
180	126	97	115	177

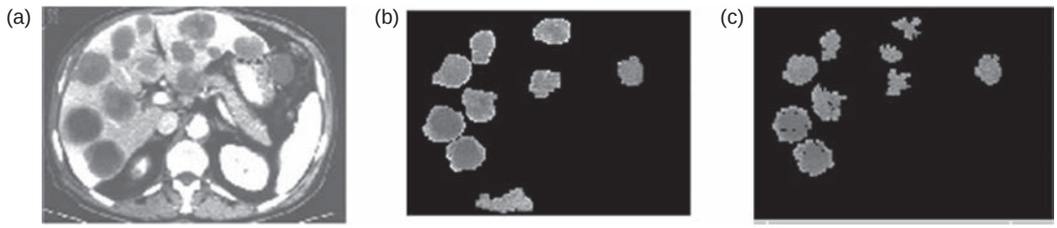

Fig. 3. (a) Input image, (b) ROI segmented by the threshold based segmentation method, (c) ROI segmented by Active contour segmentation method.

In the input image taken for analysis the tumor region is in dark intensity range and the background region in light intensity range. Pixel intensities are analyzed in three intensity ranges above 200, between 100 and 200 and below 100. As per the temperature predicted by the proposed heat prediction method, the pixel intensities below 100 need heat to be very high in the range greater than 94 °C.

For the pixel intensities in the range 100 to 200 the heat predicted is in the range between 45 °C to 94 °C. The above two conditions are region with highly infected tumor pixels which needs heat to be above 45 °C. The third range of pixel intensities are above 200, for which the heat predicted is in the range from 36.7 °C to 45 °C. The normal tissue temperature is 36.88 °C.

3.3. Analysis of Healthy and Tumor Pixels in the ROI

In the lesion taken for analyzing the pixels by threshold based segmentation, there are totally 812 pixels in the ROI. Out of the 812 pixels 595 pixels are identified to be tumor pixels as they lie in the pixel intensity range of 0 to 200. 217 pixels lie in the intensity range above 200 and therefore they are healthy pixels. Hence 73.28% of tumor pixels and 26.72% of healthy pixels are present in the ROI.

On the other hand in the lesion taken for analyzing the pixels by the Chan Vese active based segmentation, there are totally 515 pixels in the ROI. Out of 515 pixels, 491 pixels are identified as tumor pixels and 24 pixels are identified as healthy pixels. Therefore by this method as the curves are segmented more efficiently than the threshold based method, the ROI has considerably reduced in total size. Also the number of healthy pixels in the segmented region is very less and therefore efficient segmentation is assured. In the active contour segmentation method out of the total lesion size 95.34% of pixels are tumorous and only 4.66% of pixels are healthy. Therefore very less healthy pixels are identified for heat treatment. Unwanted damage to healthy pixels can be avoided by this second method of segmentation. The analysis for other lesions in the input image is tabulated. Table IV shows the percentage of healthy and tumor pixels in the input image by threshold based segmentation and Percentage of healthy and tumor pixels in the input image by Active based contour method.

In Table V the average intensity of the pixels in the region of interest for the two segmentation methods are listed. Active contour based segmentation method has reduced ROI than the other method. The average intensity of pixels in the ROI depends on the range of pixel intensities in that region.

3.4. Analysis Based on Average Intensity Value

Analysis is made based on the average intensity value for the entire lesion present in the input image.

From the Table V it is clear that in the Chan Vese method the maximum pixels lie in the range 100 to 200. And the percentage

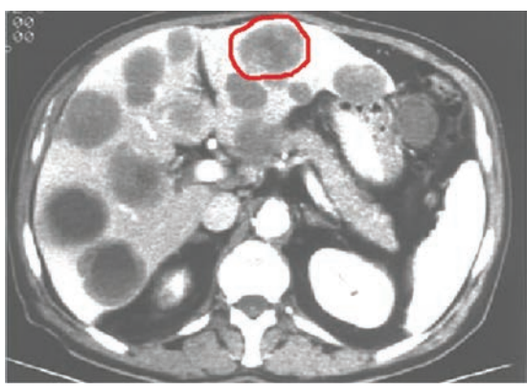

Fig. 4. The input image with a particular lesion for analysis marked red.

Table II. Analysis of ROI by threshold based segmentation method.

	Threshold based segmentation method				
Lesion number	Lesion size	Average intensity	No. of pixel intensities less than 100	No. of pixel intensities in range 100 to 200	No. of pixel intensities greater than 200
Lesion 1	812	174.37	2	593	217
Lesion 2	1380	159.73	1	1185	194
Lesion 3	1137	154.6	2	1002	133
Lesion 4	1480	141.61	17	1327	136
Lesion 5	1353	144.6	4	1184	165
Lesion 6	622	135.05	18	498	106
Lesion 7	897	176	3	688	206
Lesion 8	815	156.97	17	717	81

Table III. Analysis of ROI by Chan Vese active contour segmentation method.

	Chan Vese Active Contour segmentation method				
Lesion number	Lesion size	Average intensity	No. of pixel intensities less than 100	No. of pixel intensities in range 100 to 200	No. of pixel intensities greater than 200
Lesion 1	515	152.46	0	491	24
Lesion 2	1124	149.26	0	1073	51
Lesion 3	968	144.71	4	929	35
Lesion 4	1234	132.66	8	1178	48
Lesion 5	1157	132.55	4	1113	40
Lesion 6	537	137.3	0	515	22
Lesion 7	486	153.72	0	468	18
Lesion 8	498	148.9	0	482	16

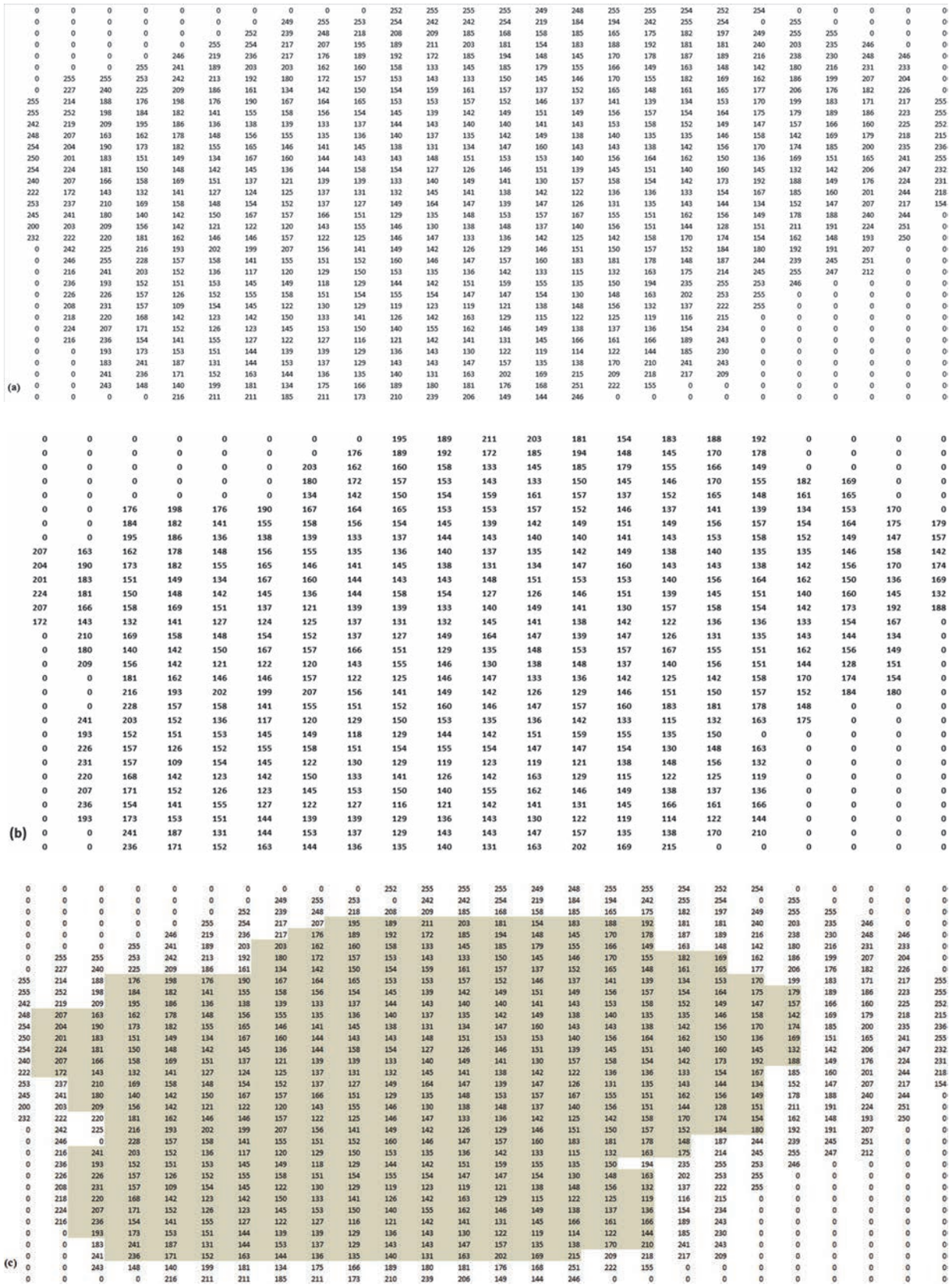

Fig. 5. (a) The grey level intensities using threshold based segmentation method. (b) The grey level intensities using active contour based segmentation method. (c) Pixel intensities common to both threshold based and Active contour based segmentation.

Table IV. Percentage of tumor and healthy pixels in ROI.

Lesion number	Percentage of tumor and healthy pixels in the ROI based on range of pixel intensities					
	Threshold based segmentation			Chan Vese active contour segmentation		
	200 to 255	100 to 200	0 to 100	200 to 255	100 to 200	0 to 100
Lesion 1	26.72	73.03	0.25	4.66	95.34	0
Lesion 2	14.06	85.87	0.07	4.54	95.46	0
Lesion 3	11.7	88.13	0.18	3.62	95.97	0.41
Lesion 4	9.19	89.66	1.15	3.89	95.46	0.65
Lesion 5	12.2	87.51	0.3	3.46	96.2	0.35
Lesion 6	17.04	80.06	2.89	4.1	95.9	0
Lesion 7	22.97	76.7	0.33	3.7	96.3	0
Lesion 8	9.94	87.98	2.09	3.21	96.79	0.8

Table V. Average intensity of pixels in the ROI.

Lesion number	Average Intensity of pixels in the ROI	
	Threshold based segmentation	Chan Vese active contour based segmentation
Lesion 1	174.37	152.46
Lesion 2	159.73	149.26
Lesion 3	154.6	144.71
Lesion 4	141.61	132.66
Lesion 5	144.6	132.55
Lesion 6	135.05	137.3
Lesion 7	176	153.72
Lesion 8	156.97	148.9

of pixels in the range above 200 is very less in Chan Vese based segmentation method than in the threshold based segmentation. Therefore we can conclude that the amount of heat predicted to be applied to the region of tumor is considerably reduced in case of proper segmentation.

3.5. Temperature Prediction for the ROI

For the input image considered the heat predicted by proposed heat prediction model is compared with the Pennes Bio heat transfer equation for the pixel intensities and shown in the Figure 6. The predicted heat values by the proposed heat prediction algorithm have shown increased values. The temperature values are tabulated in the Table VI.

The increase in the temperature values by the proposed method is due to the additional terms, variable blood perfusion and the viscosity of blood. The maximum numbers of pixel intensities lie in the pixel intensity range 100 to 255 and there are few pixels in the ROI below intensity 100.

From the Table VI the predicted heat by the proposed method is 94.469 °C for pixel intensity 100. As above this temperature the tissue boiling starts, the maximum temperature 94.469 °C is maintained for the remaining pixels intensities below 100. Tissue ablation begins from 55 °C. Tissue ablation is seen for intensities below 152 by the proposed method and below 113 by the PBHTE method.

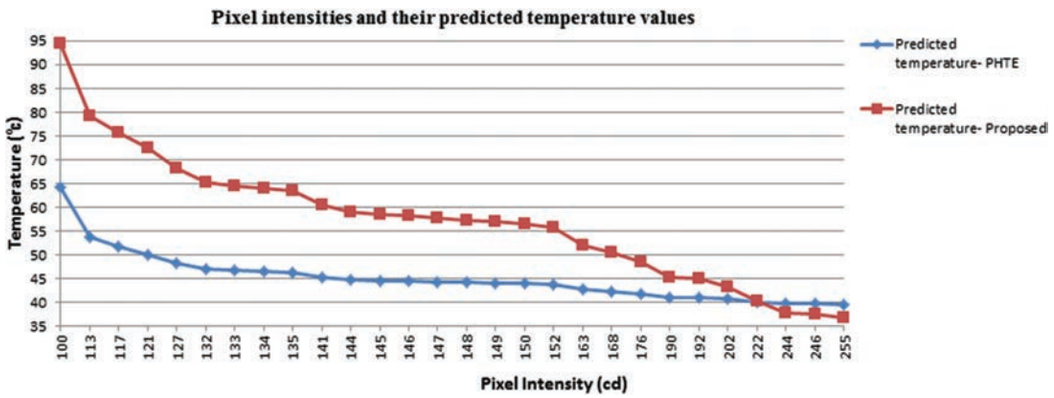

Fig. 6. Plot for the pixel intensities and their corresponding predicted temperature values.

Table VI. The predicted temperature values plotted for the pixel intensities.

Sl.no	Pixel intensity (Cd)	Predicted temperature (°C)		Sl.no	Pixel intensity (Cd)	Predicted temperature (°C)	
		PBHTE	Proposed			PBHTE	Proposed
1	100	64.336	94.469	16	148	44.234	57.3651
2	113	53.706	79.327	17	149	44.109	56.9608
3	117	51.739	75.6736	18	150	43.988	56.5647
4	121	50.13	72.4575	19	152	43.757	55.7955
5	127	48.216	68.225	20	163	42.707	52.053
7	132	46.96	65.1501	21	168	42.328	50.585
8	133	46.738	64.578	22	176	41.815	48.482
9	134	46.525	64.0189	23	190	41.123	45.395
10	135	46.319	63.4727	24	192	41.041	45.005
11	141	45.237	60.4409	25	202	40.6761	43.2152
12	144	44.778	59.0673	26	222	40.1031	40.2828
13	145	44.635	58.6285	27	244	39.6998	37.78
14	146	44.497	58.1981	28	246	39.6676	37.5812
15	147	44.363	57.777	29	255	39.5334	36.7359

4. CONCLUSION

By comparing the results of threshold based segmentation and Chan Vese Active based segmentation method, it is found that the Chan Vese Active contour based segmentation method has shown better results. Due to proper segmentation the lesion area has reduced so that the healthy pixels count in the ROI has reduced. Only the tumor pixels are segmented and so the heat to be applied unwantedly to the healthy pixels is avoided. The proposed heat prediction method predicts heat pixel wise to be applied to the tumor. From the analysis made in the input image, the total number of pixel in the ROI by threshold based segmentation is 8496. Out of this 7258 pixels are tumorous and the remaining 1238 pixels are identified as healthy pixels. Therefore 85.42% of the pixels are identified tumorous and 14.58% of pixels are healthy. By the Chan Vese based segmentation method the total number of pixels in the ROI is 6519. Out of this 6265 pixels are tumorous and remaining 254 pixels are identified as healthy pixels. Therefore 96.10% of the pixels are identified tumorous and 3.9% of pixels are healthy. From the results analyzed, Chan Vese Active contour segmentation method is found more suitable for tumor segmentation in liver. As it does the curve based segmentation the curves are segmented properly and the unwanted region predicted as ROI is reduced. In future the work can be extended and applied to other heat prediction models like Wulff Continuum model and Klinger Continuum model.

References and Notes

1. P. Golstein and G. Kroemer, Cell death by necrosis: Towards a molecular definition. *Trends Biochem. Sci.* 1, 37 **(2007)**.
2. T. J. Dubinsky, C. Cuevas, M. K. Dighe, O. Kolokythas, and J. H. Hwang, High-intensity focused ultrasound: Current potential and oncologic applications. *American J. Roentgen.* 1, 190 **(2008)**.
3. M. A. Solovchuk, T. W. H. Sheu, M. Thiriet, and W.-L. Lin, On a computational study for investigating acoustic streaming and heating during focused ultrasound ablation of liver tumor. *Appl. Therm. Eng.* 1, 62 **(2013)**.
4. H. H. Pennes, Analysis of tissue and arterial blood temperature in the resting human forearm. *J. Applied Physiology* 2, 93 **(1948)**.
5. A. B. Holbrook, J. M. Santos, E. Kaye, V. Rieke, and K. B. Pauly, Real-time MR thermometry for monitoring HIFU ablations of the liver. *Magnetic Resonance in Medicine* 2, 365 **(2010)**.
6. M. W. Dewhirist, B. L. Viglianti, M. Lora-Michiels, M. Hanson, and P. J. Hoopes, Basic principles of thermal dosimetry and thermal thresholds for tissue damage from hyperthermia. *Int. J. Hyperthermia* 3, 267 **(2003)**.
7. E. Y. K. Ng and Y. Chen, Segmentation of breast thermogram: Improved boundary detection with modified snake algorithm. *J. Mechanics in Medicine and Biology* 2, 123 **(2006)**.
8. S. C. Fok, E. Y. K. Ng, and G. L. Thimm, Computerized breast thermography: Study of image segmentation and temperature cyclic variations. *J. Medical Engineering and Technology* 1, 12 **(2001)**.
9. M. EtehadTavakol, S. Sadri, and E. Y. K. Ng, Application of K- and fuzzy c-means for color segmentation of thermal infrared breast images. *J. Medical Systems* 1, 35 **(2010)**.
10. Dayakshini and Surekha Kamath, Keerthana Prasad, and K. V. Rajagopal, Segmentation of breast thermogram images for the detection of breast cancer—A projection profile approach. *J. Image and Graphics* 1, 47 **(2015)**.
11. V. Dixit and J. Pruthi, Review of image processing techniques for automatic detection of tumor in human liver. *Int. J. of Computer Science and Mobile Computing* 3, 371 **(2014)**.
12. B. L. Davies, S. Chauhan, and M. J. S. Lowe, A robotic approach to HIFU based neurosurgery, Medical Image Computing and Computer-Assisted Intervention, Springer, Berlin, Heidelberg **(1998)**, Vol. 1496, pp. 386–396.
13. S. J. C. G. Hectors, I. Jacobs, G. J. Strijkers, and K. Nicolay, Multiparametric MRI analysis for the identification of high intensity focused ultrasound-treated tumor tissue. *PloS One* 6, 1 **(2014)**.
14. H. Rempp, R. Hoffmann, J. Roland, A. Buck, A. Kickhefel, and C. D. Claussen, Threshold-based prediction of the coagulation zone in sequential temperature mapping in MR-guided radio frequency ablation of liver tumors. *European Radiology* 5, 1091 **(2012)**.
15. Y. A. Alsultanny, Color image segmentation to the RGB and HSI model based on region growing algorithm, Recent Advances In Computer Engineering and Applications, World Scientific and Engineering Academy and Society (WSEAS), Wisconsin, USA **(2010)**, pp. 63–68.
16. A. M. Khan and S. Ravi, Image Segmentation methods: A comparative study. *Int. J. Soft Computing and Engineering* 4, 84 **(2013)**.
17. M. Ganesh and V. Palanisamy, An efficient segmentation technique for MRI medical images. *Int. J. Innovative Technology and Exploring Engineering* 5, 70 **(2012)**.
18. J. Canny, A computational approach to edge detection. *IEEE Trans. Pattern Anal. Mach. Intell.* 6, 679 **(1986)**.
19. N. N. Z. M. Rajdi, L. M. Yun, H. N. Abduljabbar, W. M. Hafizah, and J. S. Z. En, Edge detection and diameter measurement of appendiceal ultrasound images for the assessment of acute appendicitis. Advances in Environment, Biotechnology and Biomedicine, WSEAS, Czech Republic **(2012)**, pp. 330–335.
20. E. Mendi and M. Milanova, Image segmentation with active contours based on selective visual attention, *Proceedings of 8th WSEAS International Conference on Signal Processing* Istanbul, Turkey, May–June **(2009)**.
21. T. F. Chan and L. A. Vese, Active contours without edges, *IEEE Transactions on Image Processing* 2, 266 **(2001)**.
22. S. Roujol, B. D. de Senneville, S. Hey, C. Moonen, and M. Ries, Robust adaptive extended kalman filtering for real time MR-thermometry guided HIFU interventions. *IEEE Transactions on Medical Imaging* 3, 533 **(2012)**.
23. W. Wulff, The energy conservation equation for living tissue. *IEEE Transactions in Biomedical Engineering* 6, 494 **(1974)**.
24. H. G. Klinger, Heat transfer in perfused biological tissue-1. *General Theory in Bulletin of Mathematical Biology* 4, 403 **(1974)**.
25. T.-C. Shih, T.-L. Horng, K. C. Huang-wen, and H. Tzung-Chi, Numerical analysis of coupled effects of pulsatile blood flow and thermal relaxation time during thermal therapy. *Int. J. Heat and Mass Transfer* 2, 3763 **(2012)**.
26. M. Shahnazari, C. Aghanajafi, M. Azimifar, and H. Jamali, Investigation of bioheat transfer equation of pennes via a new method based on wrm and homotopy perturbation. *Int. J. Research and Reviews in Applied Sciences* 3, 306 **(2013)**.
27. P. Revathy and V. Sadasivam, Recent advances in computer science, *Proceedings of the 14th International Conference of Applied Computer and Applied Computational Science*, Kuala Lumpur, Malaysia, April **(2015)**.

Received: 7 August 2015. Revised/Accepted: 11 December 2015.